Available online at www.sciencedirect.com
ScienceDirect
Chinese Journal of Natural Medicines 2020, **18**(6): 436-445
doi: 10.1016/S1875-5364(20)30051-0
Chinese Journal of Natural Medicines

•Research article•

Sodium tanshinone IIA sulfonate prevents radiation-induced damage in primary rat cardiac fibroblasts

ZHOU Dan[1, 2], YANG Wen-Ke[3], ZHANG Yi-Fan[1, 4], XIE Jin-Hui[5], MA Li[1, 4], YANG Hui-Dong[5], LI Yi[6*], XIE Ping[1*]

[1] *Department of Cardiology, Gansu Provincial Hospital, Lanzhou 730000, China;*
[2] *School of Clinical Medicine, Gansu University of Chinese Medicine, Lanzhou 730000, China;*
[3] *School of Basic Medical Science, Lanzhou University, Lanzhou 730000, China;*
[4] *Ningxia Medical University, Yinchuan 750004, China;*
[5] *Gansu Provincial Hospital, Lanzhou 730000, China;*
[6] *School of Stomatology, Lanzhou University, Lanzhou 730000, China*

Available online 20 Jun., 2020

[ABSTRACT] This study investigated the effects of X-ray irradiation on primary rat cardiac fibroblasts (CFs) and its potential mechanism, as well as whether sodium tanshinone IIA sulfonate (STS) has protective effect on CFs and its possible mechanism. Our data demonstrated that X-rays inhibited cell growth and increased oxidative stress in CFs, and STS mitigated X-ray-induced injury. Enzyme-linked immuno-sorbent assay showed that X-rays increased the levels of secreted angiotensin II (Ang II) and brain natriuretic peptide (BNP). STS inhibited the X-ray-induced increases in Ang II and BNP release. Apoptosis and cell cycle of CFs were analyzed using flow cytometry. X-rays induced apoptosis in CFs, whereas STS inhibited apoptosis in CFs after X-ray irradiation. X-rays induced S-phase cell cycle arrest in CFs, which could be reversed by STS. X-rays increased the expression of phosphorylated-P38/P38, cleaved caspase-3 and caspase-3 as well as decreased the expression of phosphorylated extracellular signal-regulated kinase 1/2 (ERK 1/2)/ERK 1/2 and B cell lymphoma 2 (Bcl-2)/Bcl-2 associated X protein (BAX) in CFs, as shown by Western blotting. STS mitigated the X-ray radiation-induced expression changes of these proteins. In conclusion, our results demonstrated that STS may potentially be developed as a medical countermeasure to mitigate radiation-induced cardiac damage.

[KEY WORDS] Sodium tanshinone IIA sulfonate; Cardiac fibroblasts; Radiation; Oxidative Stress; Apoptosis
[CLC Number] R965 **[Document code]** A **[Article ID]** 2095-6975(2020)06-0436-10

Introduction

Radiation therapy (RT), with concurrent chemotherapy and surgery, is widely used in the treatment of cancer. Although RT greatly improves the prognosis and long-term survival of cancer patients, healthy tissue exposed to radiation close to the tumour may suffer short- and/or long-term side effects [1-3]. Among the multiple RT-induced side effects, radiation-induced heart disease (RIHD) is the primary cause of benign death in patients undergoing chest radiotherapy, and this disease may occur within a few years after the patient receives radiation [4]. RIHD is mainly characterized by asymptomatic myocardial ischaemia, acute and chronic pericarditis, accelerating atherosclerosis of coronary artery disease, conduction abnormalities, myocarditis, valvulitis and heart failure [5, 6]. Studies have shown that the cause of RIHD may be related to oxidative stress and radiation-induced apoptosis [7]. However, the mechanism of RIHD is not clear.

Cardiac fibroblasts (CFs) have multiple functions in normal or pathological conditions of the heart, such as the synthesis and deposition of the extracellular matrix and cell-cell communications with other cardiac cells, including myocytes and endothelial cells [8-10]. Cardiac fibroblasts also synthesize and secrete many bioactive molecules, including interleukins, tumour necrosis factor α (TNFα), TGFβ, angiotensin II (Ang II), endothelin 1 (ET1), and natriuretic peptides, including brain natriuretic peptide (BNP), and vascular endothelial growth factor (VEGF). The interaction of CFs with other cell types affects multiple cell signalling pathways (e.g., extracel-

[Received on] 10-Nov.-2019
[Research funding] This work was supported by the National Natural Science Foundation of China (No. 81860047), and the Postdoctoral Science Foundation of China (No. 22019M653474).
[*]**Corresponding author]** E-mail: liyilz@163.com (LI Yi); Tel: 0931-8281921, E-mail: pingxie66@163.com (XIE Ping)
These authors have no conflict of interest to declare.

lular signal-regulated kinase (ERK), c-Jun NH2-terminal protein kinase, and P38), the secretion of numerous growth factors and cytokines, microRNA exchange, gene and protein expression, and angiogenesis [11-13]. The physiological functions of cardiomyocytes in RIHD were intensively investigated over the past few decades [14-16], but little attention has been paid to CFs.

Sodium tanshinone IIA sulfonate (STS), is a water-soluble derivative of tanshinone IIA that is one of the key components isolated from *Salvia miltiorrhiza Bunge*, which is a traditional Chinese medicine used for the treatment of cardiovascular diseases [17-19]. Previous researches showed that STS had cardioprotective effects, such as the prevention of myocardial ischaemia/reperfusion injury and radiation-induced toxicity [20-22]. The possible mechanism of STS protection is thought to be the reduction of oxidative stress-triggered injury and apoptosis [23, 24]. Gu *et al.* demonstrated that STS attenuated fibrosis damage in CFs through the inhibition of ER stress and the TGF-β1/Smad pathway [25]. However, whether STS has other protective effects on CFs and its underlying mechanisms are not clear. Therefore, our research focused on the changes in CFs after radiation injury and the effects of STS on these changes.

Materials and Methods

Primary CFs isolation, culture and identification

CFs were isolated from neonatal Sprague-Dawley rats (1–3 days old) under sterile conditions. The apical tissue was washed with pre-chilled PBS after cutting with curved scissors. The pieces of the heart were digested at 37 °C with 0.25% trypsin (Gibco, Grand Island, NY, USA) for 5 min and digested with 1% collagenase II 4 to 5 times at 37 °C. The supernatant was digested for 8 min each time, and an equal volume of DMEM medium (Gibco, Grand Island, NY, USA) containing 20% fetal bovine serum (ABW, Uruguay) was added to terminate the reaction. The digested cell suspension was filtered through a 200-mesh cell sieve, and centrifuged at 250 *g* for 8 min. The supernatant was discarded, and the cells were re-suspended in DMEM medium containing 10% fetal bovine serum cultured at 37 °C in a 95% humidified atmosphere with 5% CO_2 for 90 min. The non-adherent cells were discarded, and the adherent cells were washed 3 times with PBS. Complete medium was added and replaced every 2 or 3 days. Vimentin (1 ∶ 100, Proteintech Group, Wuhan, Hubei, China) positive cells were considered CFs. The cells were passaged as they grew to 80% confluence. CFs at passage one or two were used for subsequent experiments. All experiments were performed in accordance with the guidelines of the Experimental Animal Center of Gansu University of Chinese Medicine.

Irradiation procedure

The cells were seeded with fresh culture medium and cultured for 24 h prior to radiation treatment. A single dose of 0.5, 1, 2, or 4 Gy of X-rays was administered to the cells using a Siemens PRIMUS high-energy linear accelerator (Siemens AG, Erlangen, Germany), operating at a dose-pulse rate of 6 MV·min^{-1} with a source-to-CFs distance of 100 cm. After radiation, the cells were maintained at 37 °C and 5% CO_2 cell culture incubator up to 48 h, and the culture medium was replaced every 24 h. Exposure of all samples was performed at room temperature.

Cell viability analysis

Cell viability was determined using the 3-(4, 5-dimethyl-2-thiazolyl)-2, 5-diphenyl tetrazolium bromide (MTT) assay. The experiment included a control group and STS treatment with groups (2.5, 5, 10, 20 μg·mL^{-1} for 24 h and 48 h). The purity of STS (Shanghai First Chemical Company, Shanghai, China) used in the present study was > 95%, and STS was dissolved in DMEM medium. Here, 1×10^5 cells/mL cells were seeded into 96-well plates, cultured for 12 h, and treated with 0, 0.25, 5, 10, 20 μg·mL^{-1} STS for 24–48 h. MTT (20 μL) was added to each well and incubated for 4 h. The medium was discarded and replaced with 150 μL of dimethyl sulfoxide (Sigma-Aldrich, St. Louis, MO, USA) in each well. The cultures were incubated for 10 min. The OD570 nm was measured, and the proliferation rate was calculated. Each treatment and control were assayed in at least six wells, and the cell viability is expressed as a percentage of the control cells.

Cell colony formation assay

Cell survival was measured using the colony formation assay, which was performed to determine the effect of radiation damage on CFs. Briefly, the cells were plated in 60-mm dishes at 1×10^3 cells/well in triplicate and exposed to different doses (0–4 Gy) of irradiation using an X-ray irradiator (Siemens AG, Erlangen, Germany) at a rate of 2.1 Gy/min. The treated cells were incubated in the corresponding medium for 14 days in 5% CO_2 at 37 °C. The colonies were fixed in methanol for 20 min and stained with 0.5% crystal violet (Sigma-Aldrich Corp. St. Louis, MO, USA) for 30 min. The number of colonies (≥ 50 cells) was counted using ImageJ (the National Institutes of Health, US).

Lactate dehydrogenase release assay

The effect of X-ray damage on the CFs were identified using the LDH assay. The cells were treated with 0, 0.25, 1, 2 and 4 Gy of radiation. The supernatants of the culture media were collected after 48 h to measure the amount of LDH released. The protective effect of STS on the CFs was also determined using the LDH assay. The CFs were pretreated with different dose of STS for 24 h and irradiated with the same dose X-rays. The culture medium was collected 48 h after X-ray irradiation, and LDH activity was measured using a colorimetric assay from a commercial LDH assay kit, according to the manufacturer's instructions (Nanjing Jiancheng Bioengineering Institute, Nanjing, China).

Reactive oxygen species (ROS) flow cytometric analysis

The CFs were randomly divided into various experimental and control groups prior to X-ray irradiation. The cells were divided into the following groups: 0 Gy (0 + 0 control) group; 4 Gy radiation (4 + 0) group; 4 Gy + 0.25 μg·mL^{-1}

STS (4 + 2.5) group; 4 Gy + 5 μg·mL^{-1} STS (4 + 5) group; 4 Gy + 10 μg·mL^{-1} STS (4 + 10) group; and 4 Gy + 20 μg·mL^{-1} STS (4 + 20) group. Flow cytometry was used to assess the levels of by radiation-induced ROS. Briefly, the CFs were labelled with 0.1 mmol·L^{-1} DCFH-DA (Nanjing Jiancheng Bioengineering Institute, Nanjing, China). DCFH-DA is oxidized into fluorescent DCF in the presence of ROS, which allows the ROS levels to be determined indirectly using flow cytometry.

Superoxide dismutase (SOD) and malondialdehyde (MDA) assay

Following pretreatment with different doses of STS for 24 h, the CFs were irradiated with 4-Gy X-ray. Proteins were extracted from the cells 48 h after X-ray radiation. The activity of SOD and the content of MDA in the irradiated CFs with STS treatment were determined using commercial kits according to the manufacturer's protocols (Nanjing Jiancheng Bioengineering Institute, Nanjing, China).

Enzyme-linked immuno-sorbent assay (ELISA)

To investigate the effect of STS on X-irradiation-induced CFs secretion *in vivo*, the culture medium was collected 48 h after irradiation. The cells were pretreated with different concentrations of STS. The collected supernatants were assayed for Ang II, BNP and VEGF using a rat Ang II ELISA kit, a rat BNP ELISA kit and a rat VEGF ELISA kit (Jianglai biology, shanghai, China), respectively.

Cell cycle analysis

The CFs in the logarithmic growth phase were harvested and seeded in DMEM containing 10% FBS at a density of 2 × 10^6 cells per flask. The cells were allowed to adhere, and the culture medium was removed and replaced with medium containing different concentrations of STS or control. The cells were cultured for 24 h before irradiation. The cells were cultured for 48 h after irradiation at 4 Gy, harvested, washed once with cold PBS, resuspended in 1 mL PBS, and fixed with prechilled 70% ethanol at 4 °C for 12 h. After centrifugation at 100 × *g* for 5 min, the collected cells were washed twice with PBS, resuspended in 0.5 mL of a propidium iodide staining solution and incubated at 37 °C for 30 min in the dark. Cell cycle analysis was performed using a Cell Cycle and Apoptosis Kit (Beyotime, Shanghai, China) following the manufacturer's instructions. The DNA contents of the cells were measured using a flow cytometer (BD, New Jersey, USA) at 488 nm and analyzed with Flowjo (BD, New Jersey, USA).

Cell apoptosis assays

The effect of STS on apoptosis was detected using a PE-Annexin-V/7-AAD Cell Apoptosis Kit (BD, New Jersey, USA), according to the manufacturer instructions. Briefly, after exposure to X-ray radiation for 48 h, CFs pretreated with STS or control were centrifuged to remove the medium. The cell pellet was washed with PBS twice and co-stained with 5 μL of Annexin V-PE and 5 μL of 7-AAD for 20 min at room temperature in the dark. A volume of 400 μL of 1 × Binding Buffer was added to each tube. The samples were analyzed using flow cytometry (BD, New Jersey, USA) within 1 h.

Western blot analysis

After treatment with STS or control, cells at 80% confluence were collected and washed three times with PBS. RIPA buffer was added to extract the total protein, and equal amounts of protein were loaded onto 12% sodium dodecyl sulphate-polyacrylamide gel electrophoresis (SDS-PAGE) gels for protein separation. The proteins were transferred to nitrocellulose membranes, and the membranes were blocked with 5% non-fat dried milk for 1 h. The membranes were incubated with primary antibodies (P38 at 1 ∶ 1000, p-P38 at 1 ∶ 1000, ERK 1/2 at 1 ∶ 1000, p-ERK 1/2 at 1 ∶ 1000, B cell lymphoma 2 (Bcl-2) at 1 ∶ 1000, Bcl-2 associated X protein (BAX) at 1 ∶ 1000, and cleaved caspase-3 or caspase-3 at 1 ∶ 1000) overnight at 4 °C. The membranes were washed with Tris-buffered saline (pH 7.2) containing 0.05% Tween 20 (TBST), and incubated with secondary antibodies at room temperature for 1.5 h. The membranes were washed with TBST and incubated with the enhanced chemiluminescence reagent to detect the proteins of interest. The levels of GAPDH were used as loading controls. Rabbit polyclonal antibodies for BAX, Bcl-2, P38, and ERK 1/2 were purchased from the Proteintech Group (Wuhan, Hubei, China). Antibodies for caspase-3, phosphorylated ERK 1/2, and phosphorylated P38 were purchased from Cell Signaling Technology (Beverly, MA, USA). The relative intensities were quantified using ImageJ.

Statistical analysis

Statistical analyses of the results were performed using SPSS20.0 (version 12.0; IBM, USA). The results are expressed as the means ± standard deviation (SD). Comparisons between the various levels of radiation with or without STS treatment were performed by two-way analysis of variance (ANOVA). A paired *t*-test was used to evaluate differences between the same levels of radiation versus without treatment. Comparisons between groups were performed using one-way ANOVA. *P*-values < 0.05 were considered statistically significant for all statistical analyses.

Results

Identification of primary rat CFs

Vimentin is an intermediate fibre in interstitial cells, and it is part of the cell skeleton. Vimentin maintains cell the integrity. CFs positive for vimentin expression. The results showed that vimentin-positive cells with green fluorescence were considered highly purified cardiac fibroblasts (Fig. 1).

STS increased primary rat CFs cell viability and protected CFs from X-ray damage

To observe the effect of STS on cell viability, the CFs were exposed to various concentrations of STS after 24 and 48 h. The results of the MTT assays showed that STS increased cell viability in a concentration-dependent manner. The proliferation rate was significantly increased in cells treated with 20 μg·mL^{-1} STS for 48 h ($P < 0.01$) (Fig. 2A). Our results indicated that STS had a positive effect on the vi-

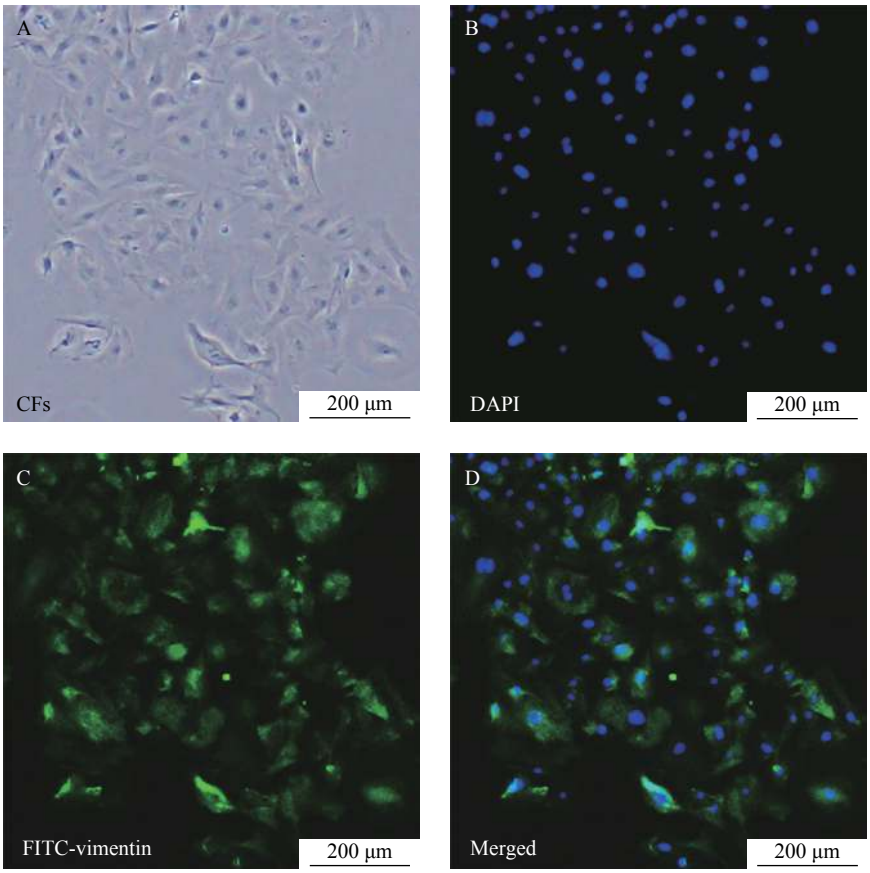

Fig. 1 The identification of CFs using immunofluorescent. (A) Representative images of CFs are shown. (B) Nuclei of CFs were stained with DAPI. (C) Vimentin staining of CFs. (D) The merged picture of (B) and (C). The same magnification (40 ×) was used for all images

ability of CFs.

To determine the optimal dose of radiation for CFs, a colony formation assay was used to evaluate the effect of irradiation on the proliferation of CFs by calculating the colony number. The results from these assays demonstrated that X-ray radiation significantly suppressed the growth of CFs in a dose-dependent manner, compared to the control cells ($P < 0.01$) (Figs. 2B, 2C). Based on a colony formation assay, a 4-Gy X-ray was selected for development of the CFs damage model in subsequent experiments.

The protective effect of STS in CFs was investigated using an LDH release assay. As shown in Fig. 2D, a marked increase in LDH activity was observed after 4-Gy X-ray exposure ($P < 0.01$). Cells treated with different doses of STS prior to exposure to 4-Gy X-ray radiation showed a decrease in LDH release with increasing STS doses. These results showed that pretreatment with STS significantly prevented radiation damage in CFs ($P < 0.01$).

STS protected against X-ray radiation-induced oxidative stress in primary rat CFs

Previous studies showed that radiation increased the production of ROS, which are key signals in the triggering of caspase-dependent apoptosis [26]. To examine the mechanisms underlying the antioxidant activity of STS, we evaluated the contents of ROS and MDA and the activity of SOD. STS suppressed ROS formation in CFs after irradiation with 4-Gy X-ray (Figs. 3A, 3B). SOD activity in the 4 + 0 radiation group was significantly decreased compared with that the 0 + 0 control group and STS increased SOD activity (Fig. 3C). The content of MDA in the 4-Gy X-ray group was higher than the 0 + 0 control group, and a decreasing trend was observed after STS intervention, However, the difference was not statistically significant. Pretreatment with STS reversed these alterations (Fig. 3D). These results indicated that STS treatment was significant inhibited X-ray radiation-induced increases in the contents of ROS and the decrease in SOD activity in CFs.

STS inhibited the secretion of Ang II and BNP of CFs after X-irradiation but not VEGF

To assess the effects of STS on the secretion of CFs, we measured the levels of Ang II, BNP and VEGF in the culture medium of CFs treated with STS and X-ray. As shown in Figs. 4A, 4B, 4-Gy X-ray increased Ang II and BNP levels, which was significantly higher than the level of the 0 + 0 control group ($P < 0.01$). After treatment with STS, the Ang II and BNP levels were significantly decreased ($P < 0.01$). There was no significant difference in BNP levels between the 4 + 0 group and the 4 + 2.5 group. However, X-irradiation did not significantly elevate VEGF levels in the culture medium. STS treatment did not significantly alter the VEGF

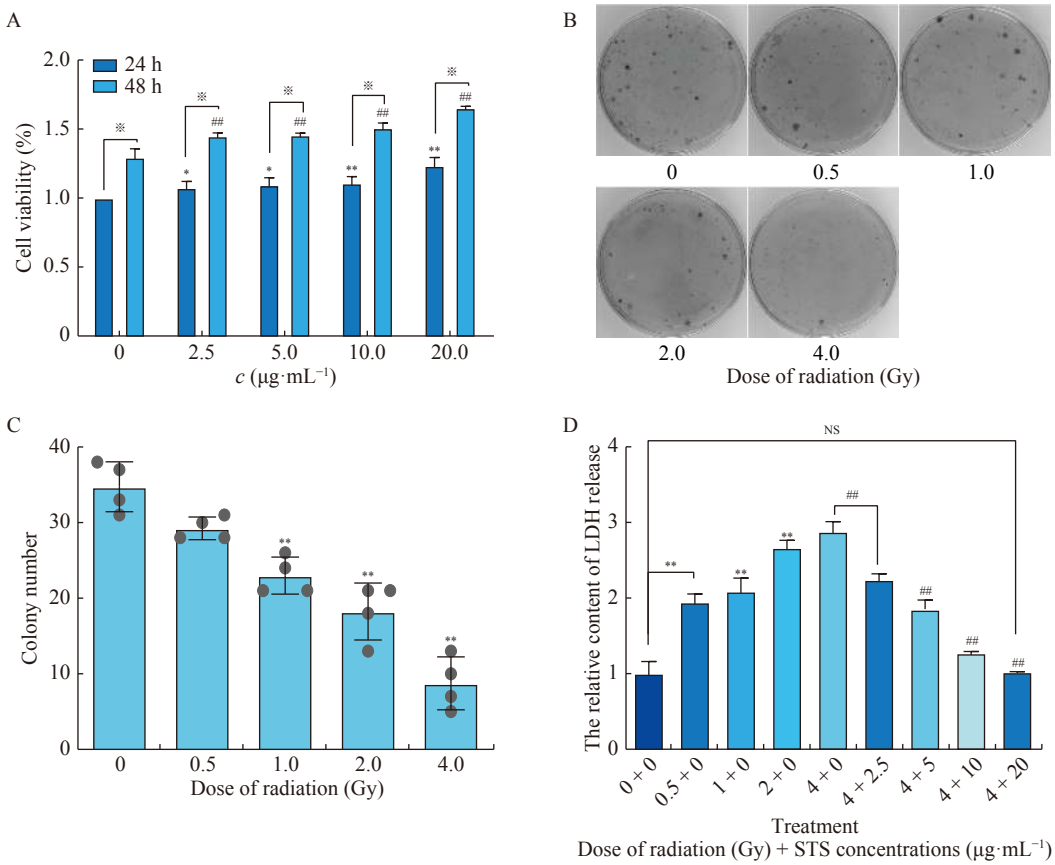

Fig. 2 The effect of radiation and STS on primary rat CFs. (A)The effects of STS on cell viability as measured by the MTT assay. $^{*}P < 0.05$, $^{**}P < 0.01$ *vs* control group at 24 h; $^{\#}P < 0.05$, $^{\#\#}P < 0.01$ *vs* control group at 48 h; $^{※}P < 0.05$ 24 h *vs* 48 h (B) Representative images of colony formation assay on CFs treated with different doses of radiation show that radiation exposure inhibited the colony-forming capacity in a dose-dependent manner. (C) The results of the colony formation assay are expressed as colony number ($n = 4$), $^{**}P < 0.01$ *vs* control group. (D)The effects of X-ray radiation and STS treatment on the LDH release of CFs were assessed using LDH release assay. $^{**}P < 0.01$ *vs* the 0 + 0 control group; $^{\#\#}P < 0.01$ *vs* the 4 + 0 group; NS, No significance. All data are expressed as mean ± SD ($n = 3$). LDH, Lactate dehydrogenase

levels (Fig. 4C).

STS reduced X-ray radiation-induced S phase cell cycle arrest in primary rat CFs

Flow cytometric analysis was performed to determine the distribution of CFs at each phase of the cell cycle. X-ray radiation-induced S phase accumulation compared with the 0 + 0 control group, and STS reduced S phase cell cycle arrest compared with the radiation group in a concentration-dependent manner. STS treatment at 5, 10, and 20 μg·mL^{-1}, significantly decreased the percentage of cells in S phase cell cycle arrest compared with the 4-Gy X-ray group ($P < 0.01$). The difference between 10 and 20 μg·mL^{-1} STS was statistically significant ($P < 0.05$) (Figs. 5A, 5B).

STS ameliorated apoptosis of primary rat CFs after X-irradiation

The percentage of apoptotic fibroblasts increased in the 4 + 0 group compared to the 0 + 0 control group ($P < 0.01$). However, after treatment with STS, the rate of apoptosis decreased to 13.50% ± 0.82% in the 4 + 20 group compared to 38.06% ± 1.61% in the 4 + 0 group ($P < 0.01$). These results demonstrated that STS alleviated X-irradiation-induced CFs apoptosis. There was no significant difference between the 0 + 0 group and 4 + 0 group. (Figs. 5C, 5D).

STS protected against the X-ray radiation-induced apoptosis of CFs via the involvement of the MAPK signaling pathway

The apoptosis assay showed that X-rays induced apoptosis in CFs and STS reduced the radiation-induced apoptosis of CFs. We next assessed X-ray radiation-induced expression changes in apoptosis-related molecules and P38 MAPK pathway-related molecules in CFs by Western blotting. X-ray radiation significantly upregulated the levels of p-P38/P38, cleaved caspase-3 and caspase-3 and downregulated the levels of p-ERK 1/2/ERK 1/2, and Bcl-2/BAX. STS treatment significantly downregulated the levels of p-P38/P38, cleaved caspase-3, caspase-3 and the ratio of cleaved caspase-3/caspase-3 and upregulated the levels of p-ERK 1/2/ERK 1/2 and Bcl-2/BAX in radiation-damaged CFs (Fig. 6).

Discussion

RIHD is one of the side effects of exposure to ionizing radiation (IR), and several therapeutic targets, including anti-inflammatory, anti-fibrotic and anti-apoptotic mediators, are

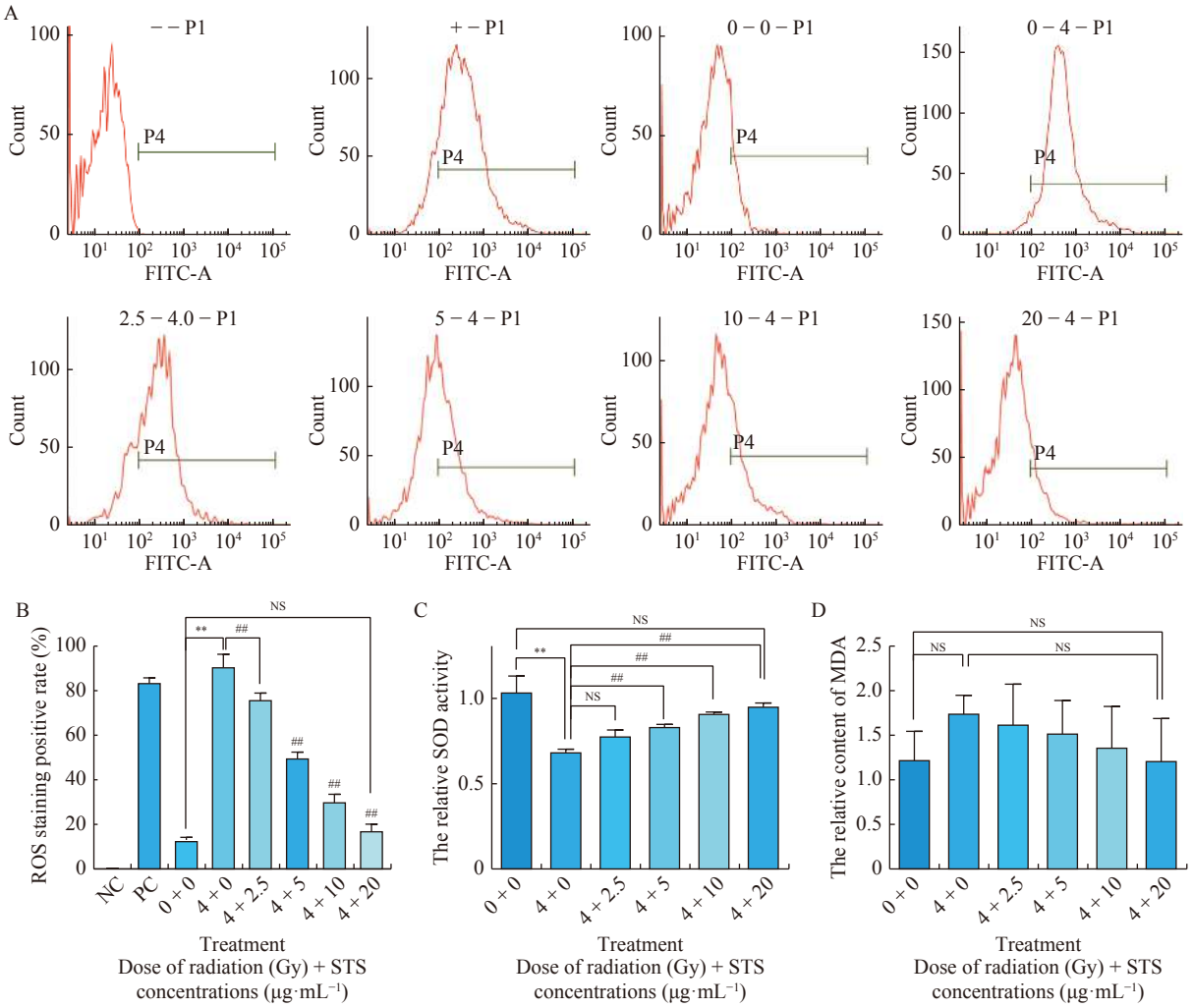

Fig. 3 STS treatment ameliorated radiation-induced CFs oxidative stress. (A) DCFH-DA labelled ROS was measured by flow-cytometry analysis. (B)The ROS staining positive rates are expressed as mean ± SD. NC, negative control. PC, positive control. (C) The relative SOD activity results in CFs. (D) The relative content of MDA results in CFs. $^{**}P < 0.01$ *vs* the 0 + 0 control group; $^{\#\#}P < 0.01$ *vs* the 4 + 0 group; NS, No significance. All data are expressed as mean ± SD ($n = 3$). ROS, reactive oxygen species; SOD, Superoxide dismutase; MDA, Malondialdehyde

being explored [27, 28]. STS is widely used to treat cardiovascular disease [29, 30]. Our previous study demonstrated that STS is beneficial for radiation-induced heart damage, most of which is concentrated in cardiomyocytes, and study demonstrated that 10 μg·mL^{-1} STS has protective effects on radiation-induced damage in H9C2 cardiomyocytes, while an inhibitory effect on cell proliferation when the concentration of STS was greater than 20 μg·mL^{-1} [21]. However, there are few studies on radiation-induced damage to CFs and whether STS has protective effects on these cells. In this study, we evaluated the effects of X-ray radiation on the biological behaviour of CFs and the protective effects of STS treatment.

X-ray radiation-induced cardiotoxicity is characterized by excessive intracellular ROS production, which may trigger oxidative stress and damage cell membrane proteins and lipids [5, 31]. MDA levels indicate membrane lipid peroxidation levels during oxidative damage, and LDH can be used as an indicator of cell injury because it leaks from cells after plasma membrane disruption. Endogenous antioxidant SOD protects cells from oxidative stress [32, 33]. Our data showed that radiation increased ROS, MDA, and LDH levels and decreased SOD content compared with control cells. In contrast, STS significantly suppressed ROS generation in CFs subjected to radiation-induced damage and promoted antioxidant stress by reducing LDH and MDA levels and increasing SOD levels. Therefore, these results suggested that radiation may cause cytotoxicity due to activation of oxidative stress, and the protective effects of STS may be related to its ability to scavenge oxygen free radicals and prevent lipid peroxidation in CFs. IR is also known to directly induce cellular DNA damage. Cell cycle checkpoints are activated after DNA damage to slow or prevent cell cycle progression to repair cells or prevent the spread of damaged genomes [34, 35]. The percentage of S phase cells significantly increased after irradiation [36, 37]. We assessed the influence of STS on cell cycle distribution of CFs. Our results suggested that radiation-induced

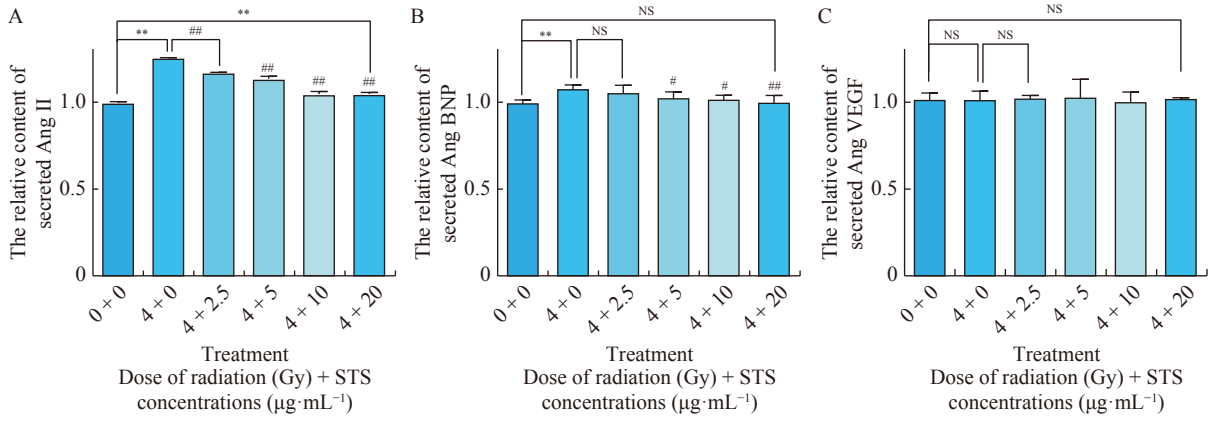

Fig. 4 The effect of X-ray radiation with or without STS on levels of Ang II (A), BNP (B) and VEGF (C) secreted by CFs. All data are expressed as mean ± SD (n = 3). $^{**}P < 0.01$ *vs* the 0 + 0 control group; $^{\#}P < 0.05$ and $^{\#\#}P < 0.01$ *vs* the 4 + 0 group; NS, No significance

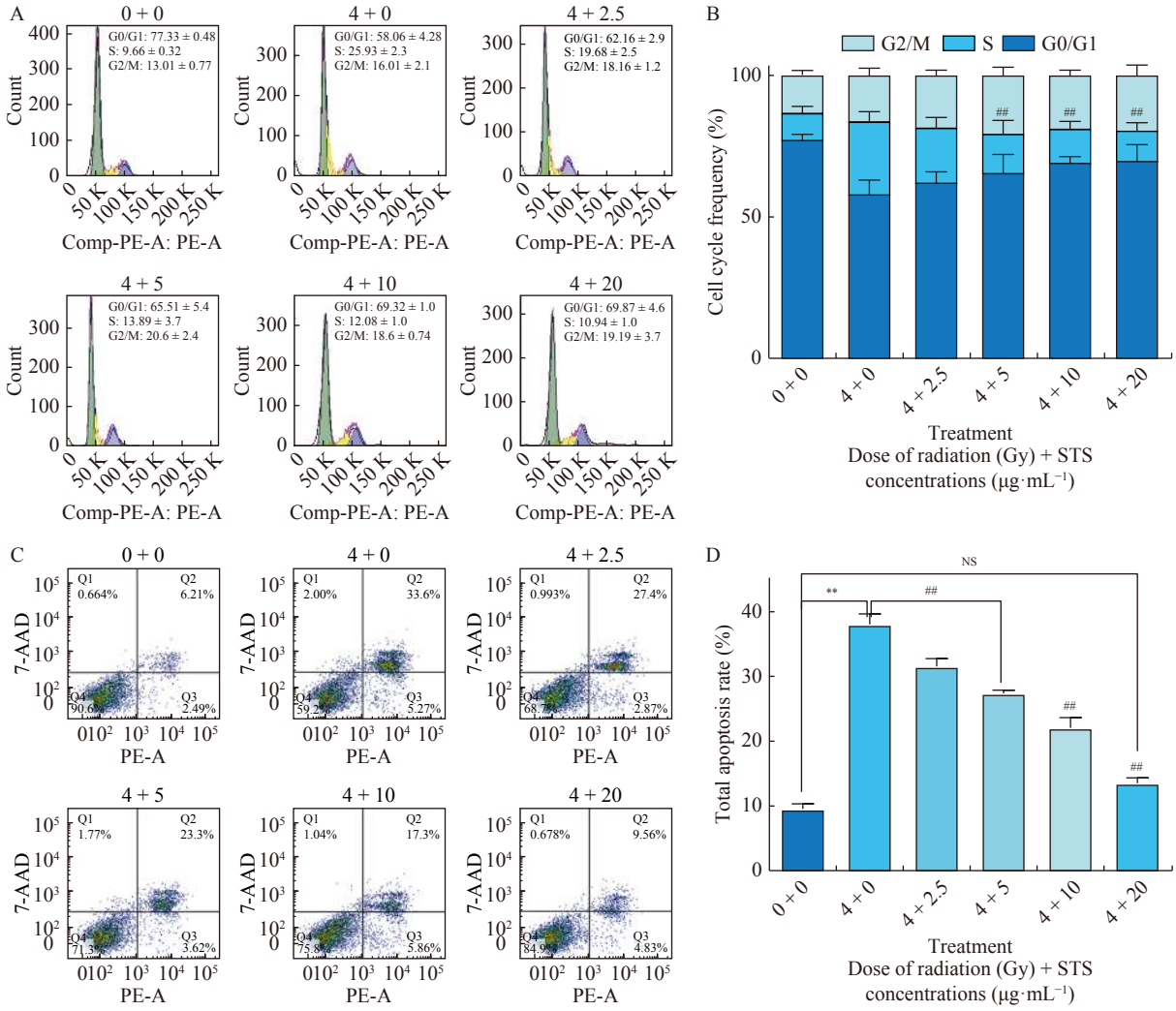

Fig. 5 The effect of X-ray radiation with or without STS on cell cycle distribution and apoptosis in CFs. (A) Representative flow cytometry graphs of the cell cycle analysis of cells irradiated with or without STS pretreatment. (B) The cell cycle analysis results of CFs are presented as means ± SD (n = 3). $^{\#\#}P < 0.01$ *vs* the S phase in 4 + 0 group. (C) The apoptosis of CFs was treated with or without STS after X-ray irradiation analysed by flow cytometry. (D) The data are expressed as mean ± SD (n = 3). $^{*}P < 0.05$ and $^{**}P < 0.01$ *vs* the 0 + 0 control group; $^{\#}P < 0.05$ and $^{\#\#}P < 0.01$ *vs* the 4 + 0 group

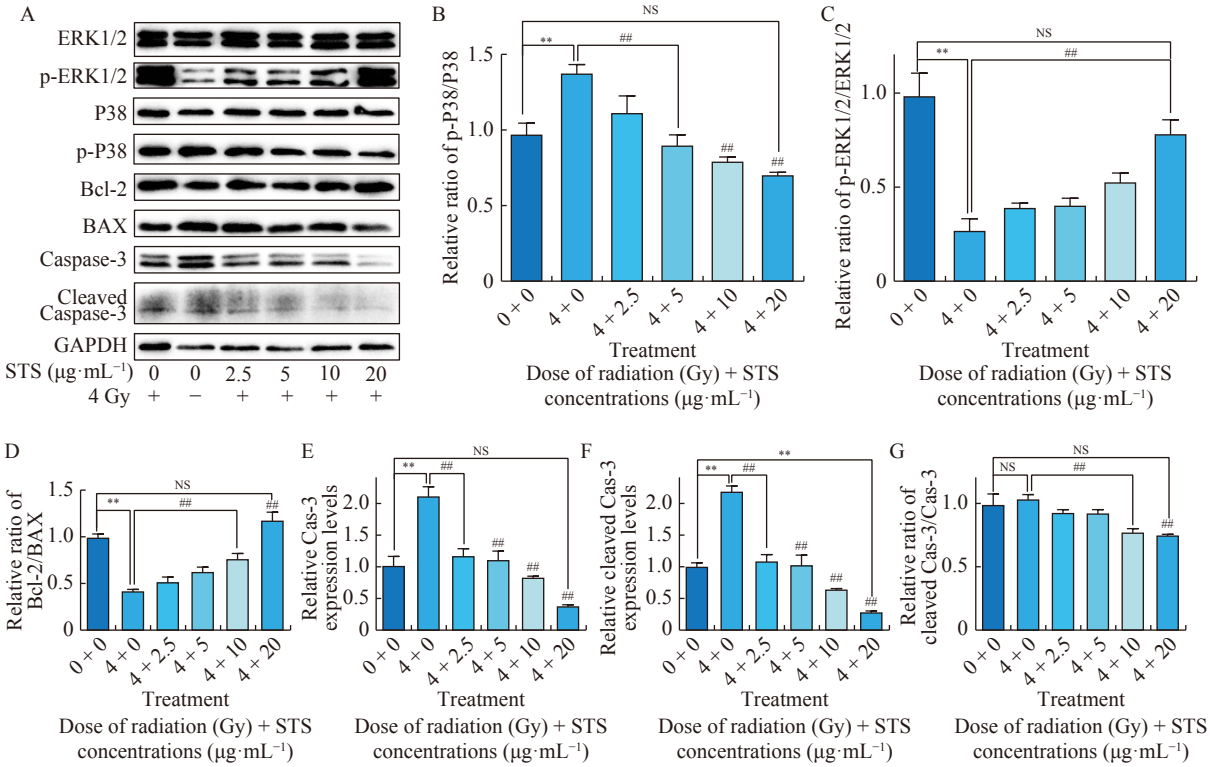

Fig. 6 STS modulated the expression of MAPK signalling pathway-associated proteins and apoptosis-related molecules after X-irradiation in CFs. (A) Representative images of the Western blotting are shown. (B) Relative ratio of p-P38/P38. (C) Relative ratio of p-ERK/ERK. (D) Relative ratio of Bcl-2/BAX. (E) Relative caspase-3 expression levels. (F) Relative cleaved caspase-3 expression levels and (G) relative ratio of cleaved caspase-3/caspase-3. GAPDH was used as a loading control. The data are expressed as mean ± SD. All experiments were repeated three times. $^{**}P < 0.01$ *vs* the 0 + 0 control group; $^{\#\#}P < 0.01$ *vs* the 4 + 0 group; NS, No significance

damage increased the proportion of cells in S phase, and STS reversed these effects, which indicates that STS can inhibit radiation-induced S phase cell cycle arrest in CFs.

CFs produce extracellular matrix (ECM) scaffolding, which is mainly used to support the adjacent cardiomyocytes, and their dynamics contribute to the proliferation, differentiation and function of cardiomyocytes, in part through the secretion of paracrine factors and markers such as TGF-*β*, Ang II, ET1, BNP and VEGF [11, 38-40]. A previous study confirmed that the STS attenuation of the radiation-induced fibrosis damage in CFs was related to the inhibition of TGF-*β* expression [25]. Upregulated Ang II also significantly increases intracellular ROS production in fibroblasts, and upregulated BNP exerts anti-proliferative effects on CFs in many heart diseases. VEGF promotes angiogenesis and collateral vessel formation [41-43]. To evaluate effects the of X-rays on the secretory function of CFs, we assessed the levels of secreted Ang II, BNP and VEGF. Our data showed that radiation significantly increased the levels of Ang II and BNP released into the medium compared to control cells, and STS treatment inhibited the release of Ang II and BNP, which suggests that radiation caused a disorder of CFs secretory function that was improved by STS. STS could improve the deteriorated heart function caused by X-rays. However, our results showed no significant difference in the effects of radiation and STS on VEGF secretion by CFs. Further research is needed to elucidate the mechanisms of these effects.

Apoptosis is an important feature of cardiotoxicity and leads to the loss of contractile units and heart failure [28, 44, 45]. In this study, the results of flow cytometry showed that X-ray radiation alone significantly increased the percentage of apoptotic cells compared with the control group. Moreover, STS ameliorated the X-ray radiation-induced apoptosis, which suggests that STS protected CFs against radiation-induced injury. MAPK is a serine-threonine protein kinase that exhibits a wide range of functions in many different cell processes. *In vitro* studies and *in vivo* evidence suggest an important role for the MAPK signalling pathway in the activation of cardiac apoptosis [11, 46]. P38 MAPK leads to apoptosis, and ERK 1/2 plays a regulatory role in cell cycle and cell proliferation, which can promote CFs proliferation. Simultaneously, the activation of ERK 1/2 is a survival factor after oxidative stress [13, 47, 48]. Previous research also confirmed that STS has a protective effect on radiation-induced injury in cardiomyocytes that involves the MAPK signalling pathway [21]. We measured the expression of MAPK signalling pathway-related proteins, including P38, ERK 1/2, p-P38 and p-ERK 1/2. Our results showed that X-ray irradiation upregulated p-P38 and downregulated p-ERK 1/2, and these results were changed by STS pretreatment. These results suggest that radi-

ation induces apoptosis by the activation of P38, and STS may activate ERK 1/2 to reduce CFs apoptosis induced by radiation and protect CFs proliferation.

P38 MAPK degrades Bcl-2 and activates BAX, which leads to apoptosis [49]. Bcl-2 inhibits the activation of BAX, which translocates to the mitochondria and releases apoptotic factors during apoptosis. An enhanced Bcl-2/BAX ratio is important for the regulation of apoptosis [28, 50, 51]. Caspase-3 is a major factor affecting apoptosis, which plays an important role in DNA fragmentation and morphological changes [52]. Previous study showed that inhibition of MAPKs may suppress apoptosis, at least partially, via the inhibition of caspase-3 activation [20]. Irradiation can induce an upregulation of BAX and caspase-3 and downregulation of Bcl-2 in cardiomyocytes, which leads to apoptosis [21, 53]. Our results showed that X-ray exposure decreases Bcl-2/BAX expression and increases cleaved caspase-3 and caspase-3 expression, and STS reverses these results. These data suggest that STS protects against the X-ray radiation-induced apoptosis of CFs via the MAPK signaling pathway.

Conclusion

We demonstrate that X-rays increases oxidative stress and apoptosis in CFs, and STS protects against radiation-induced injury. We found that the its underlying mechanism may be related to a reduced secretion of Ang II and BNP and an activation of the P38 MAPK signalling pathway. These novel findings suggest that STS is suitable as a preventive agent for X-ray-induced heart damage. We provide evidence that CFs are an important target for the pleiotropic effects of cardiovascular drugs that reduce adverse radiation-induced heart damage. Further research is needed to elucidate the specific mechanisms of STS-mediated protection of CFs from radiation-induced damage.

References

[1] Zheng HC, Onderko L, Francis SA. Cardiovascular risk in survivors of cancer [J]. *Curr Cardiol Rep*, 2017, **19**(7): 64.

[2] De Rose F, Franceschini D, Reggiori G, *et al*. Organs at risk in lung SBRT [J]. *Phys Med*, 2017, **44**: 131-138.

[3] Lee Chuy K, Nahhas O, Dominic P, *et al*. Cardiovascular complications associated with mediastinal radiation [J]. *Curr Treat Options Cardiovasc Med*, 2019, **21**(7): 31.

[4] Inami S, Abe S, Watanabe R, *et al*. Radiation-induced coronary artery disease manifested at very late phase [J]. *Int Heart J*, 2017, **58**(6): 993-997.

[5] Nabiałek-Trojanowska I, Dziadziuszko R, Wrona A, *et al*. Cardiovascular complications after radiotherapy [J]. *Cardiol J*, 2018 DOI:10.5603/CJ.a2018.0120.

[6] Yusuf SW, Venkatesulu BP, Mahadevan LS, *et al*. Radiation-induced cardiovascular disease: a clinical perspective [J]. *Front Cardiovasc Med*, 2017, **4**: 66.

[7] Cilliers GD, Harper IS, Lochner A. Radiation-induced changes in the ultrastructure and mechanical function of the rat heart [J]. *Radiother Oncol*, 1989, **16**(4): 311-326.

[8] Sullivan KE, Black LD. The role of cardiac fibroblasts in extracellular matrix-mediated signaling during normal and pathological cardiac development [J]. *J Biomech Eng*, 2013, **135**(7): 71001.

[9] Valiente-Alandi I, Schafer AE, Blaxall BC. Extracellular matrix-mediated cellular communication in the heart [J]. *J Mol Cell Cardiol*, 2016, **91**: 228-237.

[10] Banerjee I, Yekkala K, Borg TK, *et al*. Dynamic interactions between myocytes,fibroblasts, and extracellular matrix [J]. *Ann New York Acad Sci*, 2006, **1080**(1): 76-84.

[11] Frangogiannis NG. Cardiac fibrosis: cell biological mechanisms, molecular pathways and therapeutic opportunities [J]. *Mol Aspects Med*, 2019, **65**: 70-99.

[12] Espira L, Czubryt MP. Emerging concepts in cardiac matrix biology [J]. *Can J Physiol Pharmacol*, 2009, **87**(12): 996-1008.

[13] Roche PL, Filomeno KL, Bagchi RA, *et al*. Intracellular signaling of cardiac fibroblasts [J]. *Compr Physiol*, 2015, **5**(2): 721-760.

[14] Gu A, Jie Y, Sun L, *et al*. RhNRG-1beta protects the myocardium against irradiation-induced damage via the ErbB2-ERK-SIRT1 signaling pathway [J]. *PLoS One*, 2015, **10**(9): e0137337.

[15] Kim EJ, Lee J, Jung YR, *et al*. Involvement of corin downregulation in ionizing radiation-induced senescence of myocardial cells [J]. *Int J Mol Med*, 2015, **35**(3): 731-738.

[16] Zhang ZY, Li Y, Li R, *et al*. Tetrahydrobiopterin protects against radiation-induced growth inhibition in H9c2 cardiomyocytes [J]. *Chin Med J (Engl)*, 2016, **129**(22): 2733-2740.

[17] Zhou L, Zuo Z, Chow MS. Danshen: an overview of its chemistry, pharmacology, pharmacokinetics, and clinical use [J]. *J Clin Pharmacol*, 2005, **45**(12): 1345-1359.

[18] Guan R, Wang J, Li Z, *et al*. Sodium tanshinone IIA sulfonate decreases cigarette smoke-induced inflammation and oxidative stress via blocking the activation of MAPK/HIF-1alpha signaling pathway [J]. *Front Pharmacol*, 2018, **9**: 263.

[19] Qin W-W, Wang L, Jiao Z, *et al*. Lower clearance of sodium tanshinone IIA sulfonate in coronary heart disease patients and the effect of total bilirubin: a population pharmacokinetics analysis [J]. *Chin J Nat Med*, 2019, **17**(3): 218-226.

[20] Yin Y, Guan Y, Duan J, *et al*. Cardioprotective effect of Danshensu against myocardial ischemia/reperfusion injury and inhibits apoptosis of H9c2 cardiomyocytes *via* Akt and ERK1/2 phosphorylation [J]. *Eur J Pharmacol*, 2013, **699**(1-3): 219-226.

[21] Zhang W, Li Y, Li R, *et al*. Sodium tanshinone IIA sulfonate prevents radiation-induced toxicity in H9c2 cardiomyocytes [J]. *Evid Based Complement Alternat Med*, 2017, **2017**: 4537974.

[22] Pan Y, Qian JX, Lu SQ, *et al*. Protective effects of tanshinone IIA sodium sulfonate on ischemia-reperfusion-induced myocardial injury in rats [J]. *Iran J Basic Med Sci*, 2017, **20**(3): 308-315.

[23] Fu J, Huang H, Liu J, *et al*. Tanshinone IIA protects cardiac myocytes against oxidative stress-triggered damage and apoptosis [J]. *Eur J Pharmacol*, 2007, **568**(1-3): 213-221.

[24] Su CY, Ming QL, Rahman K, *et al*. *Salvia miltiorrhiza*: traditional medicinal uses, chemistry, and pharmacology [J]. *Chin J Nat Med*, 2015, **13**(3): 163-182.

[25] Gu J, Li HL, Wu HY, *et al*. Sodium tanshinone IIA sulfonate attenuates radiation-induced fibrosis damage in cardiac fibroblasts [J]. *J Asian Nat Prod Res*, 2014, **16**(9): 941-952.

[26] Kim BM, Rhee JS, Lee KW, *et al*. UV-B radiation-induced oxidative stress and p38 signaling pathway involvement in the benthic copepod *Tigriopus japonicus* [J]. *Comp Biochem Physiol C Toxicol Pharmacol*, 2015, **167**: 15-23.

[27] Musa AE, Shabeeb D. Radiation-induced heart diseases: protective effects of natural products [J]. *Medicina (Kaunas)*, 2019, **55**(5): DOI: 10.3390/medicina55050126.

[28] Spetz J, Moslehi J, Sarosiek K. Radiation-induced cardiovascular toxicity: mechanisms, prevention, and treatment [J]. *Curr Treat Options Cardiovasc Med*, 2018, **20**(4): 31.

[29] Hu Q, Wei B, Wei L, *et al*. Sodium tanshinone IIA sulfonate ameliorates ischemia-induced myocardial inflammation and lipid accumulation in Beagle dogs through NLRP3 inflamma-

some [J]. *Int J Cardiol*, 2015, **196**: 183-192.
[30] Tan D, Wu JR, Zhang XM, *et al*. Sodium tanshinone IIA sulfonate injection as adjuvant treatment for unstable angina pectoris: a meta-analysis of 17 randomized controlled trials [J]. *Chin J Integr Med*, 2018, **24**(2): 156-160.
[31] LeBaron TW, Kura B, Kalocayova B, *et al*. A new approach for the prevention and treatment of cardiovascular disorders. Molecular hydrogen significantly reduces the effects of oxidative stress [J]. *Molecules*, 2019, **24**(11): 1-26.
[32] Zhu J, Xu Y, Ren G, *et al*. Tanshinone IIA sodium sulfonate regulates antioxidant system, inflammation, and endothelial dysfunction in atherosclerosis by downregulation of CLIC1 [J]. *Eur J Pharmacol*, 2017, **815**: 427-436.
[33] Ilavenil S, Kim DH, Jeong YI, *et al*. Trigonelline protects the cardiocyte from hydrogen peroxide induced apoptosis in H9c2 cells [J]. *Asian Pac J Trop Med*, 2015, **8**(4): 263-268.
[34] Bhattacharya S, Asaithamby A. Ionizing radiation and heart risks [J]. *Semin Cell Dev Biol*, 2016, **58**: 14-25.
[35] Ishikawa K, Ishii H, Saito T. DNA damage-dependent cell cycle checkpoints and genomic stability [J]. *DNA Cell Biol*, 2006, **25**(7): 406-411.
[36] Selzer E, Hebar A. Basic principles of molecular effects of irradiation [J]. *Wien Med Wochenschr*, 2012, **162**(3-4): 47-54.
[37] Anbumani S, Mohankumar MN. Gamma radiation induced cell cycle perturbations and DNA damage in Catla Catla as measured by flow cytometry [J]. *Ecotoxicol Environ Saf*, 2015, **113**: 18-22.
[38] Dostal D, Glaser S, Baudino TA. Cardiac fibroblast physiology and pathology [J]. *Compr Physiol*, 2015, **5**: 887-909.
[39] Lajiness JD, Conway SJ. Origin, development, and differentiation of cardiac fibroblasts [J]. *J Mol Cell Cardiol*, 2014, **70**: 2-8.
[40] Chacar S, Fares N, Bois P, *et al*. Basic signaling in cardiac fibroblasts [J]. *J Cell Physiol*, 2017, **232**(4): 725-730.
[41] Chen T, Li M, Fan X, *et al*. Sodium tanshinone IIA sulfonate prevents angiotensin II-induced differentiation of human atrial fibroblasts into myofibroblasts [J]. *Oxid Med Cell Longev*, 2018, **2018**: 6712585.
[42] Lin YD, Luo CY, Hu YN, *et al*. Instructive nanofiber scaffolds with VEGF create a microenvironment for arteriogenesis and cardiac repair [J]. *Sci Transl Med*, 2012, **4**(146): 146ra109.
[43] Porter KE, Turner NA. Cardiac fibroblasts: at the heart of myocardial remodeling [J]. *Pharmacol Ther*, 2009, **123**(2): 255-278.
[44] Moore-Morris T, Cattaneo P, Puceat M, *et al*. Origins of cardiac fibroblasts [J]. *J Mol Cell Cardiol*, 2016, **91**: 1-5.
[45] Ivey MJ, Tallquist MD. Defining the cardiac fibroblast [J]. *Circ J*, 2016, **80**(11): 2269-2276.
[46] Luchetti F, Betti M, Canonico B, *et al*. ERK MAPK activation mediates the antiapoptotic signaling of melatonin in UVB-stressed U937 cells [J]. *Free Radic Biol Med*, 2009, **46**(3): 339-351.
[47] Chen LC, Shibu MA, Liu CJ, *et al*. ERK1/2 mediates the lipopolysaccharide-induced upregulation of FGF-2, uPA, MMP-2, MMP-9 and cellular migration in cardiac fibroblasts [J]. *Chem Biol Interact*, 2019, **306**: 62-69.
[48] Kuwabara M, Asanuma T, Niwa K, *et al*. Regulation of cell survival and death signals induced by oxidative stress [J]. *J Clin Biochem Nutr*, 2008, **43**(2): 51-57.
[49] Zhen AX, Piao MJ, Hyun YJ, *et al*. Purpurogallin protects keratinocytes from damage and apoptosis induced by ultraviolet B radiation and particulate matter 2.5 [J]. *Biomol Ther (Seoul)*, 2019, **27**(4): 395-403.
[50] Wu P, Du Y, Xu Z, *et al*. Protective effects of sodium tanshinone IIA sulfonate on cardiac function after myocardial infarction in mice [J]. *Am J Transl Res*, 2019, **11**(1): 351-360.
[51] Han D, Wu X, Liu L, *et al*. Sodium tanshinone IIA sulfonate protects ARPE-19 cells against oxidative stress by inhibiting autophagy and apoptosis [J]. *Sci Rep*, 2018, **8**(1): 15137.
[52] Jänicke RU, Sprengart ML, Wati MR, *et al*. Caspase-3 Is required for DNA fragmentation and morphological changes associated with apoptosis [J]. *J Biol Chem*, 1998, **273**(16): 9357-9360.
[53] Bleicken S, Wagner C, Garcia-Saez AJ. Mechanistic differences in the membrane activity of Bax and Bcl-xL correlate with their opposing roles in apoptosis [J]. *Biophys J*, 2013, **104**(2): 421-431.

Cite this article as: ZHOU Dan, YANG Wen-Ke, ZHANG Yi-Fan, XIE Jin-Hui, MA Li, YANG Hui-Dong, LI Yi, XIE Ping. Sodium tanshinone IIA sulfonate prevents radiation-induced damage in primary rat cardiac fibroblasts [J]. *Chin J Nat Med*, 2020, **18**(6): 436-445.

PhD. LI Yi has been working in the School/Hospital of Stomatology Lanzhou University since 2018. His current research focuses on the biological and mechanical coupling mechanism in pathogenesis of ischemic cardiomyopathy, cirrhosis and nonalcoholic fatty liver. Up to now, PhD. Li Yi has authored 21 scientific papers in SCI journals, and shouldered a project supported by National Natural Science Foundation of China and a project supported by Chinese Postdoctoral Science Foundation project.

Dr. XIE Ping is a Professor of Lanzhou University and Gansu University of Chinese Medicine, China; Director of Cardiovascular Research Center and Cardiovascular Medicine of Gansu Provincial Hospital (Lanzhou, China). Dr. Xie Ping is good at interventional diagnosis and treatment of coronary heart disease, radiofrequency catheter ablation of arrhythmia and permanent artificial heart pacemaker implantation. Her current research focuses on pathogenesis of radiation heart injury (RIHD) and searching for bioactive substances from natural products to cure RIHD.